ChemComm

COMMUNICATION

View Article Online
View Journal | View Issue

Cite this: *Chem. Commun.*, 2018, **54**, 2898

Received 15th November 2017,
Accepted 20th February 2018

DOI: 10.1039/c7cc08740c

rsc.li/chemcomm

SypHer3s: a genetically encoded fluorescent ratiometric probe with enhanced brightness and an improved dynamic range†

Y. G. Ermakova,[ab] V. V. Pak,[a] Y. A. Bogdanova,[a] A. A. Kotlobay,[a] I. V. Yampolsky,[a] A. G. Shokhina,[a] A. S. Panova,[ac] R. A. Marygin,[a] D. B. Staroverov,[a] D. S. Bilan,[ab] H. Sies[de] and V. V. Belousov *[abf]

We designed a genetically encoded ratiometric fluorescent probe, SypHer3s, with enhanced brightness and optimized pK_a, which responds to pH changes in different cellular compartments. SypHer3s was successfully utilized for imaging the pH dynamics in mitochondria of living neurons and in quantitative pH measurement in zebrafish embryos.

pH is a fundamental physiological parameter that is tightly regulated by a complex interaction of proton transporters, H^+-producing and consuming reactions, and buffering.[1–6] Long-term pH changes of cellular compartments can induce metabolic and signaling aberrations, cell stress and apoptosis.[7–11] Mitochondria are multifunctional organelles playing an important role in cellular energy supply,[12,13] biosynthesis,[5,14,15] and pathogenesis of many diseases like cancer, neurodegenerative disorders, and ischemic injuries.[16–20]

A number of fluorescent probes for pH monitoring in living cells have been reported. However, most of these probes have some disadvantages. For example, it is difficult to target synthetic pH sensitive dyes, such as PDMPO, BCECF and SNARF, to specific subcellular compartments, which are suitable for detecting pH changes within the narrow pH range close to their pK_a.[21]

Alternatively, a number of genetically encoded pH sensors exist including ratiometric pHluorin,[21] RaVC[22] and SypHer1/2.[23,24] Ratiometric readout not only enables quantitative calibration of the probes, but also greatly reduces the possibility of artifacts associated with changes in cellular shape and volume or cell movement during imaging.[25–27]

Brightness is an important parameter for a fluorescent probe used in live cell imaging: an increase in probe brightness decreases the excitation light intensity and exposure time, therefore minimizing phototoxic effects. The initial attempts to improve the brightness of SypHer gave rise to SypHer2, the probe with up to 3-fold enhanced fluorescence. However, the brightness of both SypHer and SypHer2 probes is still not optimal. In this study we aimed to further improve the brightness of SypHer family probes.

SypHer (HyPerC199S) is a version of the pH-sensitive hydrogen peroxide probe HyPer bearing a C199S mutation which renders the probe insensitive to hydrogen peroxide, but retains the pH sensitivity of the chromophore. To increase the brightness of the probe, we used the random mutagenesis of three existing versions of HyPer,[25,28,29] all containing the C199S mutation, followed by screening of mutants in *E. coli* libraries for brightness.

The clone selected as a result of the screening originated from SypHer and was named SypHer3s. The SypHer3s gene contains mutations Y145F, D129G (wtGFP nomenclature) and Q197L (wtOxyR nomenclature) and was 9-amino acids shorter (s = "shortened") from the N-terminus compared to the original HyPer. The Y145F mutation was previously described for GFP,[30,31] which results in an increase in the brightness of the blue-shifted variant of avGFP in combination with Y66H[30] and is known to double the fluorescence of folding reporter GFP fused to ferritin.[31] In SypHer3s this mutation is the key to increase the fluorescence in GFP-channels. The D129G and Q197L mutations accelerate the maturation rate of SypHer3s in the cytoplasm of bacterial cells of strain XL1Blue, but do not increase the fluorescence of the probe.

The fluorescence spectrum of purified SypHer3s (20 nM) exhibits two excitation maxima at 410 and 495 nm and one emission band at 525 nm (Fig. 1A). The fluorescence intensity at 410 nm decreases with an increase in pH (5.5–10.0) and the fluorescence intensity at 495 nm increases (Fig. 1A and B). The signal of the probe is measured as an F495/F410 ratio.

[a] *Shemyakin-Ovchinnikov Institute of Bioorganic Chemistry of the Russian Academy of Sciences, Moscow, Russia. E-mail: belousov@ibch.ru*
[b] *Pirogov Russian National Research Medical University, Moscow, Russia*
[c] *Department of Biochemistry, Biological Faculty, Lomonosov Moscow State University, Moscow, Russia*
[d] *Institute of Biochemistry and Molecular Biology I, Heinrich-Heine-University Düsseldorf, Düsseldorf, Germany*
[e] *Leibniz Institute for Environmental Medicine, Heinrich-Heine-University Düsseldorf, Düsseldorf, Germany*
[f] *Institute for Cardiovascular Physiology, Georg-August-University Göttingen, Göttingen, Germany*

† Electronic supplementary information (ESI) available. See DOI: 10.1039/c7cc08740c

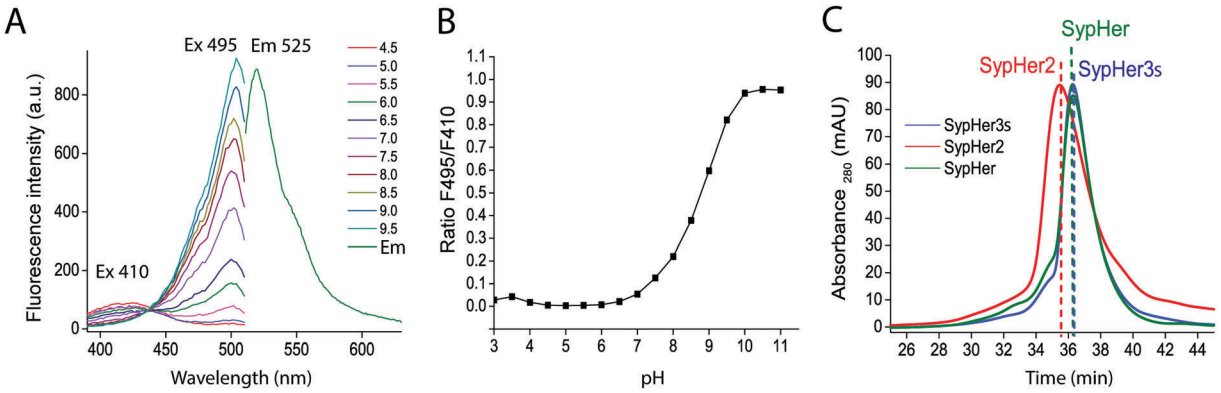

Fig. 1 SypHer3s *in vitro* characterization. (A) Fluorescence spectra of SypHer3s (20 nM) at different pH (4.5–9.5). Emission is given for pH 9.0. (B) Calibration of SypHer3s *in vitro* signal at pH (3.0–10.55) measured in buffers containing 130 mM KCl, 30 mM NaCl, 0.5 mM $MgCl_2$, 0.2 mM EGTA and (pH 3.0–4.5) 30 mM HCl–$NaH_2C_6H_5O_7$ or (pH 5.0–7.5) 15 mM KH_2PO_4–Na_2HPO_4 or 20 mM (pH 8.0–11.0) $Na_2B_4O_7$–HCl/NaOH. (C) Gel-filtration profiles of 0.02 mg mL^{-1} SypHer, SypHer2 and SypHer3s obtained using a Superdex 200 column (10 mm × 300 mm, GE Healthcare, Uppsala, Sweden) coupled to the Shimadzu chromatography system (Shimadzu Corporation, Kyoto, Japan). Eluent was 50 mM Tris–HCl, 150 mM NaCl, pH 7.5, and the flow rate was 0.4 mL min^{-1}. Absorbance was monitored at 220 nm (not shown), 280 nm, and 490 nm (not shown).

The extinction coefficient of the purified protein for SypHer3s at 495 nm (pH 7.4) is 38 012 ± 10 (M^{-1} cm^{-1}) and the quantum yield is 0.55. The extinction coefficient at 410 nm (pH 7.4) is 14 876 ± 8 (M^{-1} cm^{-1}) and the quantum yield is 0.23. Thus, the main increase in the fluorescence brightness of SypHer3 occurs due to a 2.5-fold increase in the quantum yield of the fluorescence of the sensor compared to SypHer2 at 488 nm, but there are no significant changes in the properties of the protonated form of the chromophore.

We performed gel-filtration and SDS–PAGE to evaluate the molecular mass, purity and oligomerization states of SypHer, SypHer2 and SypHer3s (Fig. 1C and Fig. S1, ESI†). The fact that SypHer3s resembles the gel-filtration profile of its parental SypHer probe confirms that none of the mutations in SypHer3s affect the oligomerization state of the probe, including those affecting the maturation speed.

To determine the extent of the fluorescence increase *in situ* we transfected HeLa-Kyoto cells with an equal amount of plasmids encoding SypHer2 and SypHer3s in three versions: the non-localized (SypHer2/3s-cyto), localized to the mitochondrial matrix of (SypHer2/3s-mito), and the mitochondrial intermembrane space (SypHer2/3s-IMS). All SypHer3s derivatives demonstrate 3.0-fold higher fluorescence at 495 nm after 24 hours post transfection compared to SypHer2 (Fig. 2A and Fig. S2A, B, ESI†).

To determine the pH sensitivity of the indicator in cultured cells we measured its F495/F410 ratio in HeLa-Kyoto cells at pH 5.5–10.5 in a buffer set containing nigericin and monensin (Fig. 2B). The F495/F410 ratio increases more than 36-fold upon changing the pH from 5.5 to 10.55 with pK_a 7.8 (Fig. 2B and Fig. S3D, ESI†). The full dynamic range is more than double that of the previous SypHer versions, and pK_a is closer to physiological cytosolic and mitochondrial matrix pH.

The fluorescence response of SypHer3s to various stimuli was studied in HeLa-Kyoto cells (Fig. 2 and Fig. S3, ESI†). Acidification of cells predominantly results from the accumulation of metabolically generated H^+ (such as that produced by

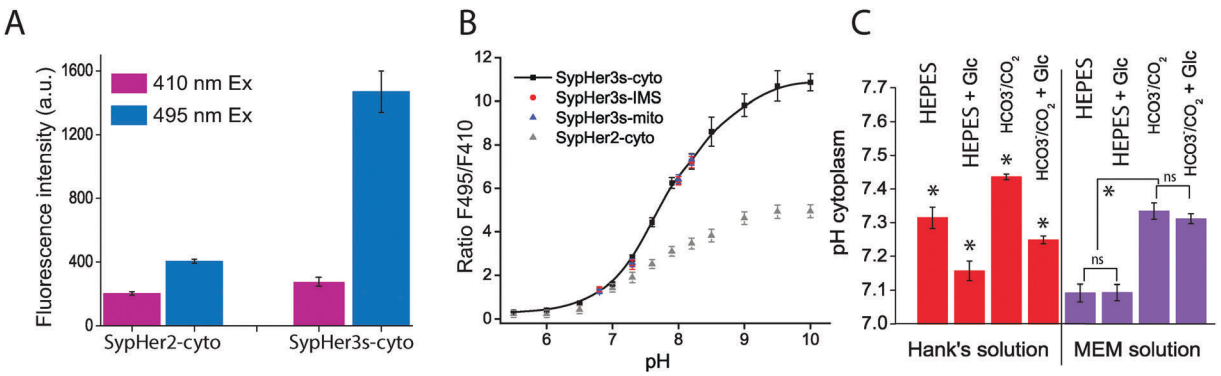

Fig. 2 Monitoring pH using SypHer3s in HeLa-Kyoto cells. (A) Fluorescence intensities of HeLa-Kyoto cells expressing cytosolic versions of SypHer2 or SypHer3s. (B) Calibration of SypHer3s targeted to the cytoplasm (cyto), mitochondrial matrix (mito) and mitochondrial intermembrane space (IMS) and SypHer-2 expressed in HeLa-Kyoto cells using nigericin and monensin containing buffers. Each point contains data from at least 100 cells. (C) Cytosolic pH of HeLa-Kyoto cells measured in Hank's solution or minimal essential medium (MEM) based solutions buffered with 20 mM HEPES or 20 mM $NaHCO_3^-/CO_2$ with or without 20 mM glucose. ns – not significant. *$P < 0.01$, one-way ANOVA, followed by Bonferroni correction and Duncan *post hoc* test. The error bars represent the s.e.m.

aerobic or anaerobic metabolism) and the extrusion of HCO_3^- from cells *via* a Cl^-–HCO_3^- anion exchanger of the SLC4 solute carrier family.[32] This suggests that the different types of buffers and different amounts of trophic substrates used for microscopy analysis of living cells will affect the pH of the cytoplasm. We performed analysis of pH_{cyt} of HeLa-Kyoto cells incubated in Hank's solution supplemented with 20 mM of HEPES buffer (Fig. S3A, ESI†) with a pH value from 6.1 to 8.1, after 20 min of incubation. Fluorescence microscopy analysis of 200 cells per group demonstrated that gradual alkalization of imaging media from 6.1 to 8.1 is reflected in the change in pH_{cyt} from 7.18 ± 0.05 to 7.65 ± 0.02.

Physiological buffering is largely carried out using a bicarbonate/CO_2 system, while in cell culture experiments artificial buffer systems are often employed, *e.g.* HEPES. Earlier experiments with perfused liver suggest that nonpermeant zwitterionic buffers like HEPES induce cytosolic alkalinization.[33] Would the intracellular pH be the same in cells supplemented with medium buffered with $NaHCO_3/CO_2$ *vs.* HEPES of the same pH remains unknown. Using SypHer3s we analyzed pH_{cyt} in media with pH 7.2 based on 20 mM $NaHCO_3/CO_2$ or HEPES buffer (Fig. 2C). We found that the cytosol of cells, incubated in HEPES-buffered media, was 0.12 ± 0.02 more acidic than that for the bicarbonate system. Addition of 20 mM glucose decreased the pH of the cytoplasm to 0.16 ± 0.03 in Hank's HEPES media and to 0.19 ± 0.03 in Hank's solution buffered with $NaHCO_3/CO_2$ (Fig. 2C), which could be explained by the activation of glycolysis and metabolite transporters.

Incubation of cells in minimum essential medium (MEM) based solution leads to decreased pH_{cyt} compared to Hank's solution, both for HEPES (7.09 ± 0.02) and $NaHCO_3/CO_2$ (7.32 ± 0.02) buffered systems (Fig. 2C). However the effect of addition of extra 20 mM glucose was not observed in MEM, likely due to the increased supplementation of cells with amino acids, vitamins and nutrient monosaccharides in MEM compared to Hank's solution. Inhibition of the glucose transporter prevented glucose-stimulated acidification (Fig. S3B, ESI†).

Cell stress with addition of 20 μM NaOH to the HEPES-based medium leads to a fast increase in pH_{cyt} to 7.66 ± 0.06 with return to the base level in 13 min, and the acidic stress caused by addition of 30 μM of HCl decreases the pH of the cytoplasm to 6.95 ± 0.03 (Fig. S3C, ESI†).

Mitochondrial matrix pH is an excellent readout of the mitochondrial activity. Due to the constant pumping out of the protons, energized mitochondria have a more alkaline matrix compared to the cytosolic pH values. SypHer3s with its pK_a of 7.8 fits well for measurements of matrix pH.

Synapses are highly active compartments with high energy demands for vesicle trafficking, mediator reuptake and biosynthesis.[34] Would synaptic mitochondria be different in their energetic state from those in non-synaptic domains such as soma?

We used fusion of synaptophysin (Sph) with red fluorescent protein tdTomato to visualize synaptic boutons (pre-synapses) and co-transfected cultured primary mouse cortex neurons with Sph-tdTomato and SypHer3s-mito to measure the pH_{mito} (Fig. S4, ESI†). 12–16 days in culture, neurons formed a network demonstrating spontaneous neuronal activity.

The spatial distribution of Sph-tdTomato was identical to the previously demonstrated pattern of Sph-GFP distribution in neurons.[35] Namely, fluorescent puncta were only visible in axons, but not in the dendrites and cell bodies, indicating proper localization. We performed co-localization analysis of Sph-tdTomato with Sph-GFP and immunochemical staining with antibodies to Sph (Fig. S5, ESI†).

Mitochondria colocalized with Sph-tdTomato have a higher pH_{mito} value than the somatic mitochondria (Fig. 3A), which indicates a higher proton gradient across the inner mitochondrial membrane and potentially more productive ATP synthesis. Treatment of neurons with uncoupler carbonyl cyanide *m*-chlorophenyl hydrazone (CCCP) led to a decrease in pH_{mito} values of both non-synaptic and synaptic mitochondria to the same value (Fig. 3B).

Treatment of neurons with bicuculline, an antagonist of $GABA_A$ receptors, which removes inhibition of spontaneous calcium oscillations, leads to a sharp increase in the amplitude and frequency of calcium oscillations, as well as a decrease in the pH_{mito} of synaptic mitochondria, and a less profound

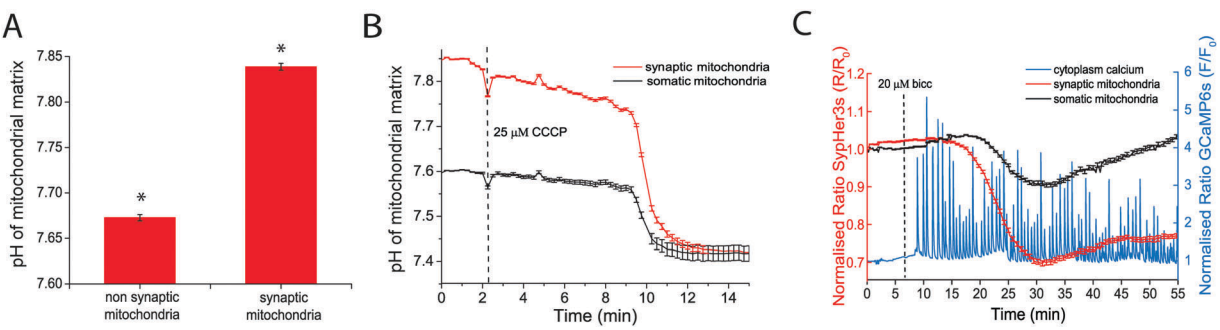

Fig. 3 pH of the mitochondrial matrix (pH_{mito}) in cultured mouse neurons. (A) Synaptic and non-synaptic mitochondrial matrix pH. Mitochondria were considered as synaptic based on their co-localization with presynaptic marker Sph-tdTomato. Non-synaptic mitochondria were those in dendrites and soma. More than 25 000 individual mitochondria counted in each group. (B) Removal of the proton gradient by addition of 5 μM CCCP. (C) pH_{mito} dynamics in neurons after 20 μM bicuculline treatment. *$P < 0.01$, one-way ANOVA, followed by Bonferroni correction and Duncan *post hoc* test. The error bars represent the s.e.m.

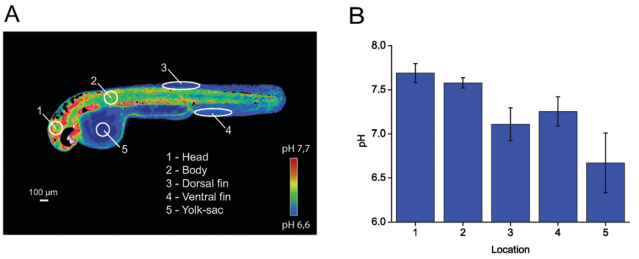

Fig. 4 SypHer3s in zebrafish *D. rerio*. (A) Image of zebrafish injected by an mRNA encoding SypHer3s biosensor at the 48 h stage. ROIs in different fish tissues indicate areas where the pH was detected. Scale bar, 100 µm. The lookup table indicates the pH values. (B) pH values in the marked areas of zebrafish. Error bars indicate standard deviation. Data on (B) are the results of 5 experiments, $N = 7$ fish.

decrease in the pH_{mito} of somatic mitochondria (Fig. 3C and Fig. S6, ESI†). This effect suggests that in the case of high synaptic activity unblocked with bicuculline, the energy demand stimulates ATP synthesis and therefore the pH gradient of the mitochondrial matrix of neurons is more rapidly depleted.

We successfully used SypHer3s *in vivo* for imaging tissue-scale gradients of pH in *D. rerio* larvae. We found that pH differs in different animal tissues (Fig. 4). The pH in the head, body, dorsal and ventral fins is 7.69 ± 0.1, 7.58 ± 0.06, 7.11 ± 0.19 and 7.25 ± 0.17, respectively (Fig. 4B). The lowest pH value was detected in the yolk sac, 6.67 ± 0.34.

In conclusion, we designed a genetically encoded fluorescent probe SypHer3s, with enhanced brightness and an elevated dynamic range around physiological pH values, capable of detecting pH-changes in living cells in the different cellular compartments. Its pK_a makes it the probe of choice for monitoring pH in the mitochondrial matrix. SypHer3s demonstrated a bright signal *in vivo* revealing pH heterogeneity in zebrafish embryo tissues. Overall, SypHer3s is an efficient tool for monitoring pH dynamics in physiological and pathological processes in living systems.

The work was supported by the following grants: Russian Science Foundation (probe development, mitochondrial and cytosolic pH imaging: 17-14-01086 to VVB; chromatography: 14-50-00131 to IVY and AAK), Russian Foundation for Basic Research (zebrafish transfection and imaging: 15-54-74003, 16-34-60175, 17-00-00214, 17-04-01690), DAAD Fellowship 57314022 and Sergey Shpiz stipend to YGE, National Foundation for Cancer Research (NFCR) to HS, and DFG IRTG 1816. We thank Matvey Roshchin and Evgeny Nikitin (Institute of Higher Nervous Activity and Neurophysiology) for providing the anti-Sph antibodies.

Conflicts of interest

There are no conflicts to declare.

Notes and references

1 P. Swietach, R. D. Vaughan-Jones, A. L. Harris and A. Hulikova, *Philos. Trans. R. Soc., B*, 2014, **369**, 20130099.
2 B. A. Webb, M. Chimenti, M. P. Jacobson and D. L. Barber, *Nat. Rev. Cancer*, 2011, **11**, 671–677.
3 R. Z. Zhan, N. Fujiwara, E. Tanaka and K. Shimoji, *Brain Res.*, 1998, **780**, 86–94.
4 D. G. Nicholls, *Eur. J. Biochem.*, 1974, **50**, 305–315.
5 P. Bernardi, *Physiol. Rev.*, 1999, **79**, 1127–1155.
6 H. H. Felle, *Ann. Bot.*, 2005, **96**, 519–532.
7 V. Labi and M. Erlacher, *Cell Death Dis.*, 2015, **6**, e1675.
8 S. Matsuyama, J. Llopis, Q. L. Deveraux, R. Y. Tsien and J. C. Reed, *Nat. Cell Biol.*, 2000, **2**, 318–325.
9 J. W. Deitmer and C. R. Rose, *Prog. Neurobiol.*, 1996, **48**, 73–103.
10 R. J. Gillies, R. Martinez-Zaguilan, E. P. Peterson and R. Perona, *Cell. Physiol. Biochem.*, 1992, **2**, 159–179.
11 C. L. Brett, D. N. Tukaye, S. Mukherjee and R. Rao, *Mol. Biol. Cell*, 2005, **16**, 1396–1405.
12 G. Kroemer, L. Galluzzi and C. Brenner, *Physiol. Rev.*, 2007, **87**, 99–163.
13 G. Szabadkai and M. R. Duchen, *Physiology*, 2008, **23**, 84–94.
14 I. Ben-Sahra, G. Hoxhaj, S. J. H. Ricoult, J. M. Asara and B. D. Manning, *Science*, 2016, **351**, 728–733.
15 S. Arnaudeau, W. L. Kelley, J. V. Walsh, Jr. and N. Demaurex, *J. Biol. Chem.*, 2001, **276**, 29430–29439.
16 M. Hoth, C. M. Fanger and R. S. Lewis, *J. Cell Biol.*, 1997, **137**, 633–648.
17 P. Nicotera and M. Leist, *Cell Death Differ.*, 1997, **4**, 435–442.
18 D. L. Schotland, S. DiMauro, E. Bonilla, A. Scarpa and C. P. Lee, *Arch. Neurol.*, 1976, **33**, 475–479.
19 S. Vyas, E. Zaganjor and M. C. Haigis, *Cell*, 2016, **166**, 555–566.
20 E. J. Lesnefsky, T. I. Gudz, C. T. Migita, M. Ikeda-Saito, M. O. Hassan, P. J. Turkaly and C. L. Hoppel, *Arch. Biochem. Biophys.*, 2001, **385**, 117–128.
21 G. Miesenbock, D. A. De Angelis and J. E. Rothman, *Nature*, 1998, **394**, 192–195.
22 T. Bagar, K. Altenbach, N. D. Read and M. Bencina, *Eukaryotic Cell*, 2009, **8**, 703–712.
23 D. Poburko, J. Santo-Domingo and N. Demaurex, *J. Biol. Chem.*, 2011, **286**, 11672–11684.
24 M. E. Matlashov, Y. A. Bogdanova, G. V. Ermakova, N. M. Mishina, Y. G. Ermakova, E. S. Nikitin, P. M. Balaban, S. Okabe, S. Lukyanov, G. Enikolopov, A. G. Zaraisky and V. V. Belousov, *Biochim. Biophys. Acta*, 2015, **1850**, 2318–2328.
25 D. S. Bilan, L. Pase, L. Joosen, A. Y. Gorokhovatsky, Y. G. Ermakova, T. W. Gadella, C. Grabher, C. Schultz, S. Lukyanov and V. V. Belousov, *ACS Chem. Biol.*, 2013, **8**, 535–542.
26 Z. M. Ying, Z. Wu, B. Tu, W. Tan and J. H. Jiang, *J. Am. Chem. Soc.*, 2017, **139**, 9779–9782.
27 G. H. Aryal, L. Huang and K. W. Hunter, *RSC Adv.*, 2016, **6**, 76448–76452.
28 V. V. Belousov, A. F. Fradkov, K. A. Lukyanov, D. B. Staroverov, K. S. Shakhbazov, A. V. Terskikh and S. Lukyanov, *Nat. Methods*, 2006, **3**, 281–286.
29 K. N. Markvicheva, D. S. Bilan, N. M. Mishina, A. Y. Gorokhovatsky, L. M. Vinokurov, S. Lukyanov and V. V. Belousov, *Bioorg. Med. Chem.*, 2011, **19**, 1079–1084.
30 R. Heim and R. Y. Tsien, *Curr. Biol.*, 1996, **6**, 178–182.
31 J. D. Pedelacq, S. Cabantous, T. Tran, T. C. Terwilliger and G. S. Waldo, *Nat. Biotechnol.*, 2006, **24**, 79–88.
32 V. A. Ruffin, A. I. Salameh, W. F. Boron and M. D. Parker, *Front. Physiol.*, 2014, **5**, 43.
33 H. Sies, G. Noack and K. H. Halder, *Eur. J. Biochem.*, 1973, **38**, 247–258.
34 Julia J. Harris, R. Jolivet and D. Attwell, *Neuron*, 2012, **75**, 762–777.
35 S. Okabe, A. Miwa and H. Okado, *J. Neurosci.*, 2001, **21**, 6105–6114.